

Selectively activated PRP exerts differential effects on tendon stem/progenitor cells and tendon healing

Journal of Tissue Engineering
Volume 10: 1–14
© The Author(s) 2019
Article reuse guidelines:
sagepub.com/journals-permissions
DOI: 10.1177/2041731418820034
journals.sagepub.com/home/tej



Jianying Zhang¹, Daibang Nie¹ , Kelly Williamson¹, Jorge L Rocha¹,
MaCalus V Hogan¹ and James H-C Wang^{1,2,3} 

Abstract

To understand the variable efficacy with platelet rich plasma (PRP) treatments for tendon injury, we determined the differential effects of proteinase-activated receptor (PAR)1- or PAR4-activated PRP (PAR1-PRP, PAR4-PRP) from humans on human patellar tendon stem/progenitor cells (TSCs) and tendon healing. We show that PAR1-PRP released VEGF, whereas PAR4-PRP released endostatin. Treatment of TSCs with PAR1-PRP increased collagen I expression and matrix metalloproteinase-1 (MMP-1), but cells treated with PAR4-PRP increased less collagen I and higher MMP-2 expression. The wound area treated with PAR4-PRP formed tendon-like tissues with well-organized collagen fibers and fewer blood vessels, while PAR1-PRP treatment resulted in the formation of blood vessels and unhealed tissues. These findings indicate that differential activation of PRP leads to different effects on TSCs and tendon healing. We suggest that based on acute or chronic type of tendon injury, selective activation of PRP should be applied in clinics in order to treat injured tendons successfully.

Keywords

TSCs, PRP, PAR1, PAR4, healing

Date received: 25 October 2018; accepted: 28 November 2018

Introduction

Tendon injuries are prevalent in occupational and athletics populations; however, the multistage healing process of cell proliferation and matrix production is slow in tendon injuries and results in collagen-rich scar tissue formation with poor mechanical properties resulting in a healed tendon prone to reinjury.^{1–3} Treatment strategies that can improve the quality of healing tendon are highly desirable. One popular treatment strategy for tendon injuries is the use of platelet rich plasma (PRP) because it can be used as a naturally conductive scaffold with a reservoir of growth factors that function well as an anti-inflammatory treatment.^{4–7} In order to ensure PRP as a valid treatment option, steps must be taken to understand how growth factors contained within PRP function at the injury site.

To prepare PRP, platelets (PLTs) are typically activated using thrombin. As a result of activation, PLTs release alpha granules containing a wide variety of factors involved in

many physiological functions, such as wound repair, coagulation, inflammation, angiogenesis, and malignancy.⁸ Particularly, factors released by alpha granules include both pro- and anti-angiogenic mediators, for example, VEGF and endostatin, respectively, as well as pro-angiogenic factors matrix metalloproteinases (MMP)-1 and MMP-2.⁸ Both MMP-1 and MMP-2 have been studied extensively for their

¹MechanoBiology Laboratory, Department of Orthopaedic Surgery, University of Pittsburgh School of Medicine, Pittsburgh, PA, USA

²Department of Bioengineering, University of Pittsburgh School of Medicine, Pittsburgh, PA, USA

³Department of Physical Medicine and Rehabilitation, University of Pittsburgh School of Medicine, Pittsburgh, PA, USA

Corresponding author:

James H-C Wang, MechanoBiology Laboratory, Department of Orthopaedic Surgery, University of Pittsburgh School of Medicine, 210 Lothrop Street, BST, E1640, Pittsburgh, PA 15213, USA.
Email: wanghc@pitt.edu



roles in excessive scarring, with MMP-1 expressed at low levels while MMP-2 is highly expressed in scar tissue.⁹ The pro-angiogenic VEGF is found to be highly expressed in cells from fetal and injured human tendons.¹⁰ The anti-angiogenic factor endostatin, a proteolytic fragment of collagen XVIII, is also involved in maintaining a largely avascular tendon tissue.¹¹

These pro- and anti-angiogenic factors are stored in different subsets of alpha granules in PLTs, and their secretion is differentially regulated by selective commitment of thrombin receptors, specifically proteinase-activated receptor (PAR)1 and PAR4.^{12–14} To date, most studies have incorporated the use of thrombin to activate PRP that causes the widespread release of PLT factors.¹⁵ However, the broad release of PLT factors in response to thrombin stimulation presents several challenges that may alter the healing process and the end results of PRP application for tendon injuries. Being pro- and anti-angiogenic, respectively, VEGF and endostatin may differentially affect wound healing; therefore, their selective release by activation of their corresponding receptor is essential for proper healing through the release of alpha granules containing either one or the other.¹⁴ This differential release of pro- and anti-angiogenic factors could contribute to the variable healing results of PRP treatment for tendons and other tissues.

Several studies have suggested that PRP may enhance healing of injured tendons by increasing tenocyte number and promoting collagen type I and III production,^{16,17} but tendon also consists of tendon stem/progenitor cells (TSCs) that respond to various biochemical and biomechanical stimuli, and undergo differentiation into tenocytes and proliferate, thus imparting an important role in tendon regeneration.^{18,19} Previously, we showed that PRP treatment induces differentiation of TSCs into tenocytes that are activated to proliferate and produce abundant collagen.¹⁶ Moreover, TSCs promote PRP healing in collagenase-induced rat Achilles tendinopathy, possibly by means of improved TSC differentiation toward the tenocyte lineage.²⁰ Previous research has shown that a combination of both TSCs and PRP treatment has synergic effects on rat Achilles tendon injury healing.²¹

In this study, we investigated whether the selective activation of human PLTs with either PAR1 or PAR4 can have differential effects on the release of VEGF and endostatin, and whether selective activation of human patellar TSCs using PAR1- or PAR4-activated PRP can have differential effects on TSC morphology, differentiation, proliferation, cellular collagen production, and gene expression. We also used a window defect rat model to further analyze the differential wound healing effects of PAR1- and PAR4-activated human PRP (PAR1-PRP and PAR4-PRP). Our studies show that PAR1-PRP and PAR4-PRP preparations differentially release VEGF and endostatin, and have differential effects on human TSCs in terms of morphology,

differentiation, cell proliferation, gene expression (collagen I, MMPs), and collagen production. In addition, PAR1-PRP and PAR4-PRP display differential wound healing characteristics in a rat acute injury model. Overall, our data show that stimulating PLTs with different treatments of either PAR1-PRP or PAR4-PRP resulted in different healing effects. With our data, we hope to further elucidate the differential effects seen in PRP treatments on tendon injuries.

Materials and methods

Chemicals and reagents

Thrombin from bovine plasma was obtained from Sigma-Aldrich (Cat. No. T4648-10KU, Sigma-Aldrich, St. Louis, MO). Activating peptides for PAR1 and PAR4 were obtained from Tocris Bioscience (Cat. No. 1464, 3494, Avonmouth, Bristol, UK). The other reagents used in this study will be described in the following experiments.

PLT preparation

PLTs were prepared from whole blood of 19 healthy human donors ranging in age from 19 to 51 years (9 female, 10 male). The protocol for obtaining blood samples was approved by the University of Pittsburgh Institutional Review Board. Each 9 mL of whole blood was mixed with 1 mL of 3.8% sodium citrate in a centrifuge tube and centrifuged at 500 g for 10 min. The supernatant (PRP) was transferred to a new centrifuge tube and centrifuged at 2000 g for another 10 min. The resulting supernatant was retrieved as platelet-poor plasma (PPP). The PLT-containing pellet was washed with a Tyrodes-HEPES buffer (Cat. No. AAJ67607K2, VWR, Radnor, PA) and centrifuged to remove washing buffer. The pellet was resuspended in Tyrodes-HEPES buffer to obtain PLT working solution (PLT solution).

PLT activation

Each 5 μ l of 1 mM PAR1 or PAR4 peptide was added to 100 μ l of the human PLT solution (10^7 PLTs) and mixed gently. PAR1 peptide and PAR4 peptide activated PLT are referred to as PAR1-PLT and PAR4-PLT, respectively. The PAR1-PLT or PAR4-PLT mixture was incubated at 25°C for 10 min, and centrifuged at 1000 g for 10 min. The supernatant was collected and used for the following experiments. The same volume of PLT solution activated by 5 μ l of 10 U/ μ l of bovine thrombin (Total 50 U) was used as a positive control and the PLT solution without activation (treated with 5 μ l of Tyrodes-HEPES buffer) was used as a negative control. Both controls were treated with the same procedures used for the PAR1-PLT and PAR4-PLT mixtures.

Assessing VEGF and endostatin expression in PLTs by immunostaining

Each 100 μ l of the human PLT solution was seeded in a well of a 96-well plate (10^7 PLTs/well) and incubated with 5 μ l of 1 mM PAR1 or 5 μ l of 1 mM PAR4 or 5 μ l of 10 U/ μ l thrombin or 5 μ l of Tyrodes-HEPES buffer (resting human PLTs) at 25°C for 10 min. Mouse anti-VEGF antibody (1:350, Abcam, Cat. No. ab1316, Cambridge, MA) or rabbit anti-endostatin antibody (1:350, Abcam, Cat. No. ab3453, Cambridge, MA) was added to each well and incubated at room temperature for 2 hrs. The liquid was removed by a vacuum desiccator. The PLTs were washed thrice, with 50 μ l of 0.9% saline solution each time, and the wash buffer was removed by a vacuum desiccator. The PLTs were incubated either with Cy3-conjugated goat anti-mouse IgG second antibody (1:500, Millipore, Cat. No. AP124C, Burlington, MA) at room temperature for 2 hrs for determining VEGF or FITC-conjugated goat anti-rabbit IgG second antibody (1:500, Abcam, Cat. No. ab6717, Cambridge, MA) at room temperature for 2 hrs for determining endostatin. The expression of VEGF and endostatin in PLTs treated with four different conditions was examined under a fluorescent microscope.

Measuring the release of VEGF and endostatin from PLTs by enzyme-linked immunosorbent assay

The levels of VEGF and endostatin after human PLT activation in each supernatant of above experiments were obtained using an enzyme-linked immunosorbent assay (ELISA) kit (R&D Systems, Cat. No. DVE00 for human VEGF, Cat. No. DNST0 for human endostatin, Minneapolis, MN) according to the manufacturer's protocol.

Assessing the effects of PAR1-PRP and PAR4-PRP on human TSCs in vitro

Cell morphology and proliferation—human patellar TSCs were derived from 7 healthy donors (age 28 ± 6.7 years) following our published protocol.²² Briefly, after removing the tendon sheath and surrounding paratenon, the middle portion of tendon tissue was minced into small pieces and digested with 3 mg collagenase type I and 4 mg dispase in 1 mL of PBS for 1 hr at 37°C. The suspension was centrifuged at 1500 g for 15 min, and the cell pellet was resuspended in DMEM with 1% penicillin and streptomycin and cultured at 37°C with 5% CO₂. After 2 weeks, the cells that form colonies, a typical characteristic of stem cells, were separated and identified as TSCs. They were expanded and the cells at passage 2 were seeded into 12-well plates (2×10^5 cells/well) and cultured in four different conditions, that is, Group-1: growth medium (DMEM with 1% penicillin and streptomycin) with 10% FBS (**FBS**);

Group-2: growth medium with 10% PPP, 10^7 PLTs, and 10 μ l of 1000 U/mL thrombin (**Thr-PRP**); Group-3: growth medium with 10% PPP, 10^7 PLTs, and 10 μ l of 5 mM PAR1 (**PAR1-PRP**); Group-4: growth medium with 10% PPP, 10^7 PLTs, and 10 μ l of 5 mM PAR4 (**PAR4-PRP**). After 5 days, the morphology of the cells cultured in the above four conditions was examined under a microscope. The medium was collected from each well for collagen production analysis using a Sircol kit (Biocolor Life Science Assays, Cat. No. S1000, Carrickfergus, County Antrim, UK) according to the manufacturer's protocol. The cells were detached by trypsin and the cell numbers in each well were counted by an automatic cell counter (Cellometer Auto T4, Nexcelom Bioscience LLC, Lawrence, MA). The cell proliferation was measured by population doubling time (PDT) as described previously.²³

Collagen expression and production—human TSCs were treated with the same above procedures in 12-well plates for 5 days. After removing the medium, the cells were washed thrice with PBS, and incubated with rabbit anti-collagen I antibody (1:500, Cat. No. Ab34710, Abcam, Cambridge, MA) overnight at 4°C. The next morning, the cells were washed with PBS 5 times, and incubated with Cy3-conjugated goat anti-rabbit IgG second antibody (1:1000, Cat. No. AP132C, Millipore, Billerica, MA) for 2 hrs at room temperature. Then the cells were washed with PBS for another 5 times. Finally, the cells were also counterstained with H33342 (5 μ g/mL, Cat. No. B2261, Sigma, St. Louis, MO) for 5 min. The stained cells were examined using fluorescence microscopy (Nikon, eclipse, TE2000-U).

TSC differentiation assessed by qRT-PCR—the effect of human PAR1-PRP and PAR4-PRP on the differentiation of human patellar TSCs was investigated using quantitative real-time RT-PCR (qRT-PCR). Briefly, TSCs at passage 2 were seeded in 6-well plate and cultured with the following five different conditions. Group-1: the TSCs were culture in growth medium (DMEM with 1% penicillin and streptomycin) with 10% FBS (**FBS**); Group-2: growth medium with 10% PPP and 10^7 PLTs (**PRP**); Group-3: growth medium with 10% PPP, 10^7 PLTs, and 10 μ L of 1000 U/mL thrombin (**Thr-PRP**); Group-4: growth medium with 10% PPP, 10^7 PLTs, and 10 μ L of 5 mM PAR1 (**PAR1-PRP**); Group-5: growth medium with 10% PPP, 10^7 PLTs, and 10 μ L of 5 mM PAR4 (**PAR4-PRP**). After 5 days, the culture medium was removed from each well and the cells were washed with PBS once. The RNA was extracted from the cells of each well by RNeasy Mini Kit (Qiagen, Cat. No. 74104, Waltham, MA) and 1 μ g of total RNA was used for cDNA synthesis by a SuperScript II kit (Invitrogen, Cat. No. 18064014, Carlsbad, CA). Each 100 ng RNA was used for gene analysis with SYBR Green PCR kit (QIAGEN, Cat. No. 204243, Carlsbad, CA) using a Chromo 4 Detector (MJ Research, Maltham, MA). The PCR reaction was performed at 94°C for 5 min, followed by 40 cycles of a

Table 1. Human primers used for qRT-PCR analysis.

Gene	Primer sequence	Reference
Collagen I	F: 5'-CAC CGA CCA CGA AAC CAC CG-3' R: 5'-AGC AAT ACC AGG AGC ACC AT-3'	Theret et al. ²⁴
Collagen II	F: 5'-TTT CCC AGG TCA AGA TGG TC-3' R: 5'-TCA CCT GGT TTT CCA CCT TC-3'	Zhang et al. ²⁶
MMP-1	F: CTG AAG GTG ATG AAG CAG CC-3' R: AGT CCA AGA AAT GGC CGA G-3'	Konttinen et al. ²⁵
MMP-2	F: GCG ACA AGA AGT ATG GCT TC-3' R: TGC CAA GGT CAA TGT CAG GA-3'	Konttinen et al. ²⁵
LPL	F: 5'-GAG ATT TCT CTG TAT GGC ACC-3' R: 5'-CTG CAA ATG AGA CAC TTT CTC-3'	Zhang et al. ²⁶
Runx-2	F: 5'-ACG ACA ACC GCA CCA TGG-3' R: 5'-CTG TAA TCT GAC TCT GTC CT-3'	Zhang et al. ²⁶
GAPDH	F: 5'-GGG CTG CTT TTA ACT CTG GT-3' R: 5'-TGG CAG GTT TTT CTA GAC GG-3'	Zhang et al. ²⁶

three-temperature program of 1 min at 94°C, 40 seconds at 57°C, and 40 seconds at 72°C. Finally, the reaction was terminated after a 10-min extension at 70°C. The human-specific primers were synthesized by Invitrogen (Carlsbad, CA) and used for tenocyte-related gene collagen type I, non-tenocyte-related genes collagen II for chondrocytes, Runx-2 for osteocytes, LPL for adipocytes, and MMPs testing and Glyceraldehyde 3-phosphate dehydrogenase (GAPDH) served as an internal control (Table 1).²⁴⁻²⁶

Healing of injured tendons in an acute injury rat model

A rat tendon window defect model was used to investigate the differential wound healing effects of human PAR1-PRP and PAR4-PRP. Eight rats were anesthetized, and the patellar tendon was wounded (1 × 2 mm² window defect) as described previously.²⁷ The rats were divided into four groups (two rats/group) with the four different wound treatments. Group-1: the wounds were treated with 60 μL saline (**Saline**); Group-2: treated with 10⁷ of PLT in 50 μL of PPP with 10 μL M thrombin (**Thr-PRP**); Group-3: treated with 10⁷ of PLT in 50 μL of PPP with 10 μL of 5 mM PAR1 (**PAR1-PRP**); Group-4: treated with 10⁷ of PLT in 50 μL of PPP with 10 μL of 5 mM PAR4 (**PAR4-PRP**). After surgery, the rats were allowed to recover in cages without restricting their movements. At 8 weeks, the wound areas were photographed and the rats were then sacrificed for histochemical analysis of the healed tendons.

Histological analysis of rat tendons

The effect of human PAR1-PRP and PAR4-PRP on wounded rat patellar tendon healing as described above was determined by histological analysis according to previous descriptions.³ Briefly, patellar tendons were dissected from the rats and immersed in frozen section medium (Neg 50; Richard-Allan Scientific; Kalamazoo,

MI). They were cut into 10-μm sections and dried overnight at room temperature, rinsed in PBS, and fixed in 4% paraformaldehyde for 30 min. Finally, the sections were washed in PBS, stained with hematoxylin and eosin (H&E), Safranin O, and Fast Green. The images were visualized and photographed through a microscope.

Statistical analysis

All data were obtained from at least three replicates and presented as mean ± SD.

For statistical analysis, student's *t*-test was used for comparison of two groups. For more than two groups, one-way analysis of variance (ANOVA) was used, followed by Fisher's least significant difference (LSD) test for multiple comparisons with statistical significance set at $p < 0.05$.

Results

Differential release of VEGF from vesicles of PAR1- and PAR4-activated PLTs

In resting PLTs, VEGF and endostatin are located inside vesicles. PLTs were activated by either PAR1 or PAR4 to determine the specific release of VEGF and endostatin. Thrombin was used as a positive control. The resting PLTs did not release VEGF as evidenced by more than 93% of VEGF found inside the vesicles of PLTs without treatment (Figure 1(a) and (b), white arrows), however, thrombin-activated PLTs released high levels of VEGF (Figure 1(c) and (d), yellow arrows). Similarly, PAR1-activated PLTs released a significant amount of VEGF as evidenced by the large size of PLTs with an empty center (Figure 1(e) and (f), blue arrows), while PAR4-activated PLTs did not release VEGF in an amount similar to the resting control (Figure 1(g) and (h), green arrows). Semi-quantification results indicated that more than 90% of PLTs released VEGF when they were activated by PAR1, and more than

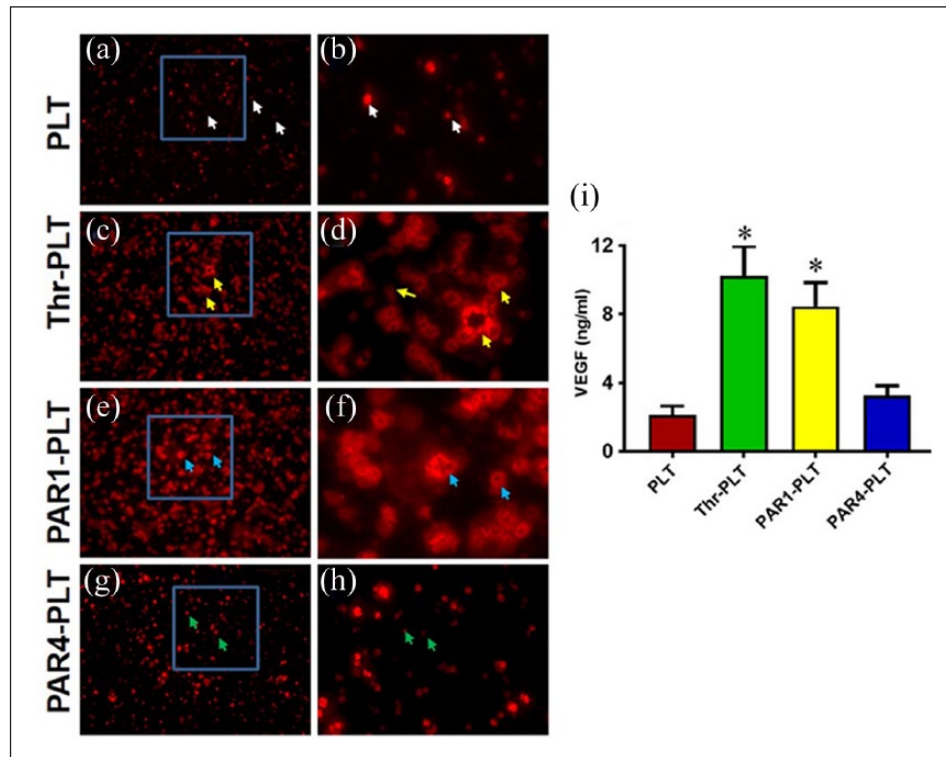


Figure 1. VEGF is released from vesicles in PAR1-activated PLTs but not in PAR4. (a) PLTs without treatment. The resting PLTs do not release VEGF as evidenced by more than 90% of VEGF found inside the vesicles of PLTs without treatment (white arrows). (b) Enlarged blue box area in (a) showing resting PLTs do not release VEGF (white arrows). (c) Activation with positive control, thrombin, releases VEGF (yellow arrows). (d) Enlarged blue box area in (c) showing substantial release of VEGF by thrombin (yellow arrows). (e) PAR1-PLTs release VEGF (blue arrows). (f) Enlarged blue box in (e) showing VEGF release by PAR1, as evidenced by large size of PLTs with empty center part (blue arrows), same as in (d). (g) PAR4-PLTs do not release VEGF (green arrows). (h) Enlarged image of blue box in (g) showing that PAR4 does not release VEGF (green arrows). (i) Semi-quantification of VEGF release in the PLTs shows that 92% of PLTs release VEGF when they are activated by thrombin, and 87% of PLTs liberate VEGF when they are activated by PAR1. However, only 4% and 7% of VEGF are released when PLTs are not activated and are activated by PAR4, respectively. * $p < 0.01$, with respect to resting PLTs.

85% of PLTs liberated VEGF when they were activated by thrombin (Figure 1(i)). However, less than 4% of PLTs released VEGF when they were not activated, and less than 7% of PLTs released VEGF when they were activated by PAR4 (Figure 1(i)). Collectively, these data indicate that VEGF was differentially released when PLTs were activated by peptides for PAR1 and PAR4.

Differential release of endostatin from vesicles of PAR1- and PAR4-activated PLTs

The opposite results of VEGF were seen with endostatin, namely, the triggered release in response to PAR4 activation. The resting PLTs did not release endostatin as evidenced by more than 86% of endostatin found inside the PLTs without treatment (Figure 2(a) and (b), white arrows). The positive control thrombin released a significant amount of endostatin (Figure 2(c) and (d), red arrows), while PAR1 treatment did not release endostatin (Figure 2(e) and (f), yellow arrows). However, high levels of

endostatin were released when PLTs were activated with PAR4 (Figure 2(g) and (h), blue arrows) as evidenced by the large size of PLTs with an empty center part. Semi-quantification results indicated that more than 86% of PLTs released endostatin when they were activated either by PAR4 or thrombin (Figure 2(i)); however, less than 11% of PLTs released endostatin when they were not activated (Figure 2(i)), or less than 13% of PLTs released endostatin when activated by PAR1 (Figure 2(i)). The results indicate that endostatin was released from PLTs at different levels in response to different activating peptides for PAR1 and PAR4.

Differential levels of VEGF released from PAR1 and PAR4-activated PLTs

The differential release levels of VEGF from PLTs activated by PAR1 and PAR4 was confirmed by ELISA. The resting PLTs did not release VEGF, as evidenced by a low level (2.3 ng/mL) found in the medium of the PLTs without

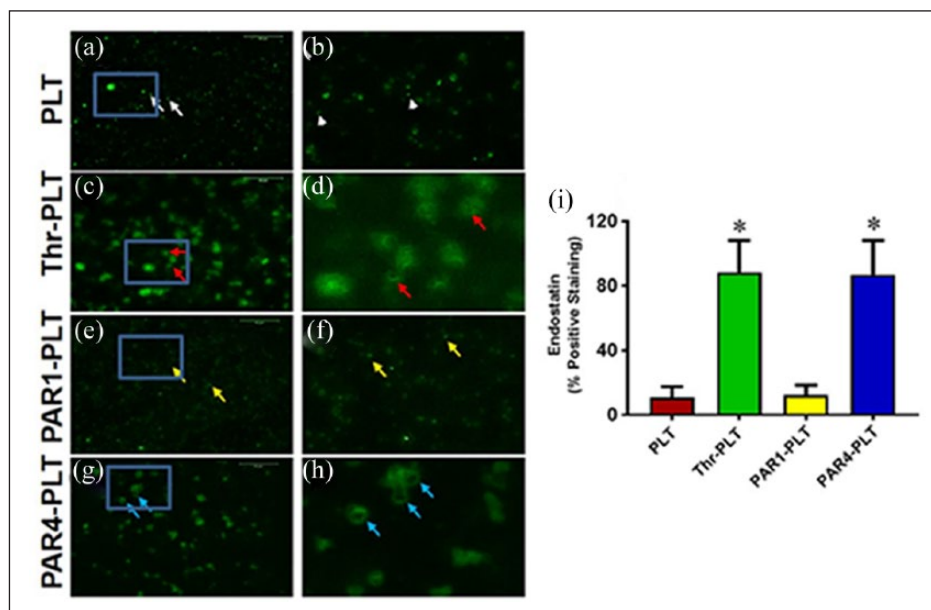


Figure 2. Endostatin is released from vesicles in PAR4-activated PLTs but not in PAR1. (a) PLTs without treatment. The resting PLTs do not release endostatin as evidenced by more than 85% of endostatin found inside the vesicles of PLTs without treatment (white arrows). (b) Enlarged blue box area in (a) showing resting PLTs do not release endostatin (white arrows). (c) Activation with positive control, thrombin, releases endostatin (red arrows). (d) Enlarged blue box area in (c) showing substantial release of endostatin by thrombin (red arrows). (e) PAR1 does not induce release of endostatin (yellow arrows). (f) Enlarged blue box in (e) showing no release of endostatin by PAR1 activation. (g) PAR4 induces release of endostatin (blue arrows). (h) Enlarged image of blue box in (g) showing that PAR4 releases endostatin as evidenced by large size of PLTs with empty center part (blue arrows) similar to that in (d). (i) Semi-quantification of endostatin release in the PLTs shows that 88% of PLTs release endostatin when they are activated by thrombin, and 87% of PLTs liberate endostatin when they are activated by PAR4. However, only 11% and 13% of endostatin are released when PLTs are not activated and are activated by PAR1, respectively. * $p < 0.01$, with respect to resting PLTs.

treatment (Figure 3(a)). Higher concentrations of VEGF were released (7.2 ng/mL) when PLTs were activated by PAR1 similar to that induced by thrombin (7.4 ng/mL), while PAR4 did not induce any VEGF (Figure 3(a)) with a level very much comparable to that in resting PLTs.

Differential levels of endostatin released from PAR1 and PAR4-activated PLTs

The differential release levels of endostatin in PLTs activated by PAR1 and PAR4 were confirmed by ELISA. The resting PLTs and PAR1 treated PLTs did not release endostatin into the medium, as evidenced by a low level of endostatin found in the medium of respective PLTs (Figure 3(b)). PAR4 did induce release of higher concentrations of endostatin (~ 5-fold compared to control) similar to the level induced by thrombin (Figure 3(b)).

Differential effects of PAR1-PRP and PAR4-PRP on cell morphology and proliferation

Human TSCs exhibit the typical cobblestone shape when they were cultured in DMEM with 10% FBS (Figure 4(a)). However, the TSCs apparently differentiated into elongated tenocyte-like cells, when they were cultured with

thrombin-activated PRP (Figure 4(b)). PAR1-PRP induced the apparent differentiation of TSCs into tenocyte-like cells and also caused the formation of “vessel-like” cellular pattern (Figure 4(c)). PAR4-PRP promoted the apparent differentiation of TSCs into tenocyte-like cells in a more organized fashion compared to PAR1-PRP (Figure 4(d)). By performing gene analysis, we confirmed that PAR1-PRP and PAR4-PRP indeed promoted differentiation of TSCs into tenocytes (Figure 5(a) and (d)). The measurement of population doubling time (PDT) indicated that the differentiated TSCs grew much faster (~twice faster) in all the PRP-containing media than in the FBS-containing medium (Figure 4(e)).

Differential effects of PAR1-PRP and PAR4-PRP on gene expression

The collagen type I gene expression was 7.2 times higher in TSCs when they were cultured in thrombin activated PRP-containing medium, 4.5 times higher with PAR1-PRP-containing medium, and 3.3 times higher with PAR4-PRP-containing medium than that of control TSCs (Figure 5(a)). MMP1 and MMP2 were both significantly increased in TSCs when they were cultured with thrombin-activated PRP-containing medium compared to the control (FBS-containing DMEM medium; Figure 5(b) and (c)).

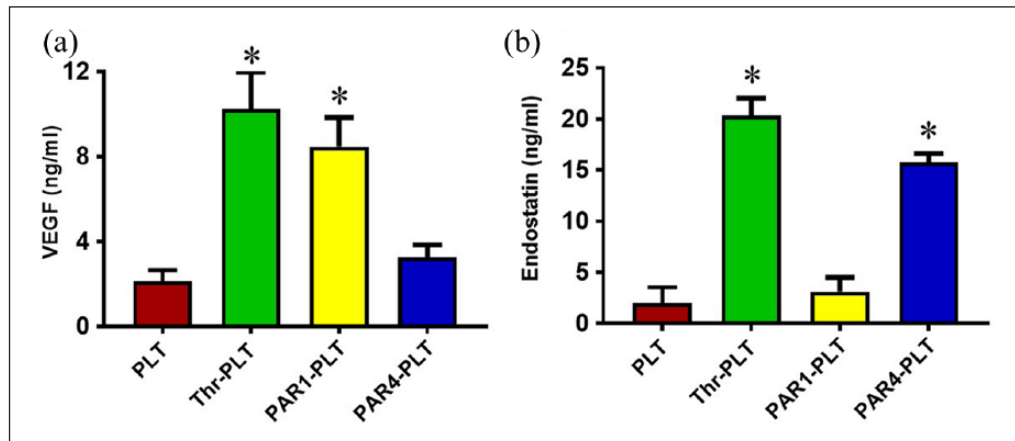


Figure 3. Selective release of VEGF and endostatin by PAR1- and PAR4-activated PLTs. (a) A significant amount of VEGF is released by PAR1-activated PLTs but not by PAR4-activated PLTs. Quantification of the amount of VEGF secreted by PLTs when activated by PAR1 shows 7.2 ng/mL VEGF, which is comparable to that released by thrombin-activated PLTs (7.4 ng/mL). However, in PAR4-activated PLTs only 2.2 ng/mL of VEGF is seen, which is similar to the amount in untreated PLTs (2.3 ng/mL). * $p < 0.01$, with respect to resting PLTs. (b) A significant amount of endostatin is secreted by PAR4-activated PLTs but not in PAR1-activated PLTs. Quantification of the amount of endostatin secreted by PAR4-activated PLTs shows 15 ng/mL endostatin, which is comparable to the amount released by thrombin-activated PLTs (15.4 ng/mL). However, in PAR1-activated PLTs, only 3.2 ng/mL of endostatin is secreted, which is similar to untreated PLTs (3.7 ng/mL). * $p < 0.01$, with respect to resting PLTs.

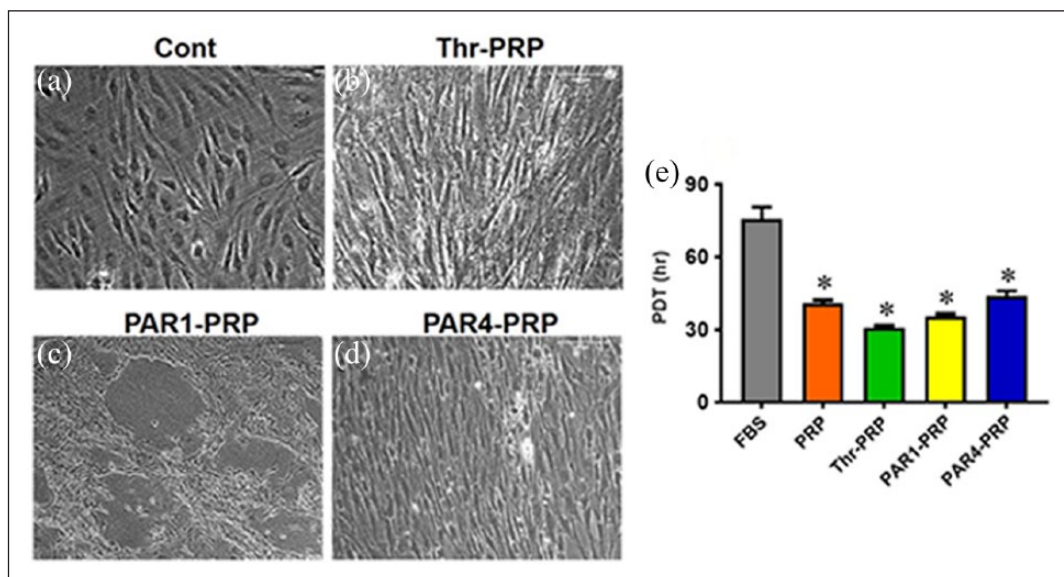


Figure 4. PAR1-PRP and PAR4-PRP differentially affect cell morphology and proliferation of human TSCs. (a) Human TSCs show their typical cobblestone shape when cultured in DMEM with 10% FBS. (b) When cultured in DMEM containing thrombin-activated PRP, TSCs exhibit elongated spindle shape, suggesting that they have differentiated into tenocytes. (c) In the DMEM containing PAR1-PRP, TSCs also apparently differentiate into tenocytes, which form a “vessel-like” pattern. (d) In the medium containing PAR4-PRP, however, TSCs become more elongated than that in Thr-PRP group (b). They are also organized in a highly parallel fashion. Moreover, the measurement of population doubling time (PDT) shows that the differentiated TSCs proliferate significantly faster in PRP-containing media than FBS-containing medium, and PAR1-PRP induced proliferation is faster than PAR4 (e). * $p < 0.01$, with respect to control group (FBS).

MMP-1 was also increased in cells with PAR1-PRP medium (3-fold increase over the control), but not in cells with PAR4-PRP medium (Figure 5(b)). Although MMP-2 did not increase in cells with PAR1-PRP medium, it was increased (3.4-fold) in cells with PAR4-PRP medium compared to

untreated control (Figure 5(c)). Finally, the expression of non-tenocyte-related genes, collagen II, Runx-2, and LPL were determined in TSCs cultured in various activation media. None of these genes were increased significantly compared to control (Figure 5(d)).

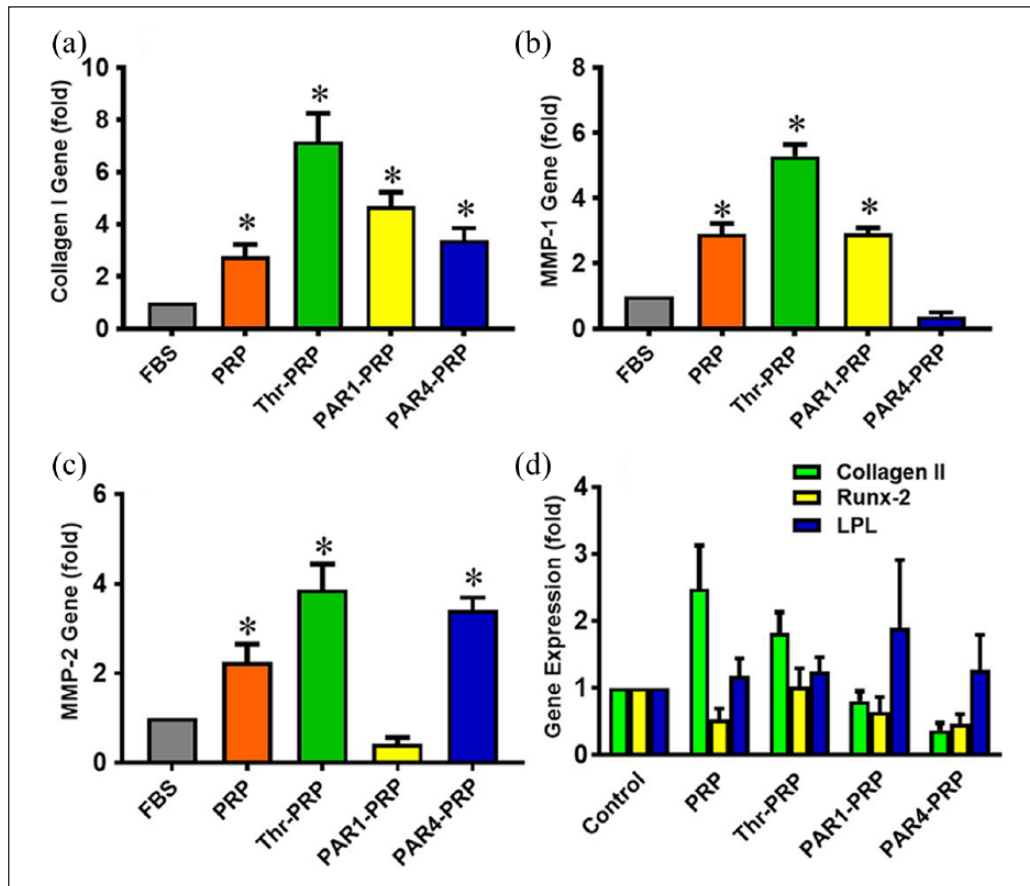


Figure 5. Differential gene expression in TSCs treated with PRP-containing media. (a) Collagen I gene expression is enhanced in TSCs cultured in different PRP containing media; it is 3-, 7-, 5-, and 3- fold greater in PRP alone, Thr-PRP, PAR1-PRP, and PAR4-PRP, respectively, than in FBS as control. (b) MMP-1 expression is also enhanced in all groups except in the PAR4-PRP group. There is a 3-, 5-, and 3-fold increase in PRP alone, Thr-PRP, and PAR1-PRP, respectively. (c) Except in PAR1-PRP, MMP-2 gene expression is enhanced in all three groups with respect to the control group (FBS). There is a 2-, 4-, and 3- fold increase in PRP alone, Thr-PRP, and PAR4-PRP, respectively. (d) For all groups, namely, PRP along, Thr-PRP, PAR1-PRP, and PAR4-PRP, the expression of three non-tenocyte-related genes (collagen II, Runx-2, and LPL) is not significantly changed. * $p < 0.05$, with respect to control (FBS).

Differential effects of PAR1-PRP and PAR4-PRP on collagen type I

High level of collagen I was expressed extensively in human patellar TSCs when they were cultured in DMEM with 10% FBS (Figure 6(a)), Thr-PRP (Figure 6(b)), and PAR1-PRP (Figure 6(c)). However, the collagen I expression was low in the cells treated with PAR4-PRP (Figure 6(d)). The Sircol assay results showed that the TSCs cultured with all PRP-containing media produced more collagen (about 2 times greater in PRP-, 5 times in thrombin-, 3 times in PAR1-, but only 1.6 times in PAR4-activated media) than those cultured in FBS alone (Figure 6(e)).

Differential effects of PAR1-PRP and PAR4-PRP on tendon healing

The differential wound healing effects of PAR1 and PAR4 were assessed on a rat patellar tendon acute injury model.

At 2 months post-injury, a large unhealed wound area was visible in untreated rats (Figure 7(a)). The thrombin-activated PRP treatment, which was used as a positive control group, resulted in that the wound healed almost completely (Figure 7(b)). This was not the case for PAR1-PRP treatment, nor PAR4-PRP treatment (Figure 7(c) and (d)). Moreover, some vessel-like tissues were found in the healing site of PAR1-PRP group (Figure 7(c)), but very few blood vessels were found in the healing site of PAR4-PRP group (Figure 7(d)).

Histological results further confirmed the above findings. In the untreated control, a large unhealed wound area was found 2 months' post-injury (Figure 8(a) and (b)). The thrombin-activated PRP treated wound healed almost completely; however, a scar-like tissue with overgrowth was observed in this group (black arrows in Figure 8(c) and (d)). Some blood vessel-like tissues were found in the healing site treated with PAR1-PRP as well as unhealed tissue characterized by a similar tissue structure seen in the

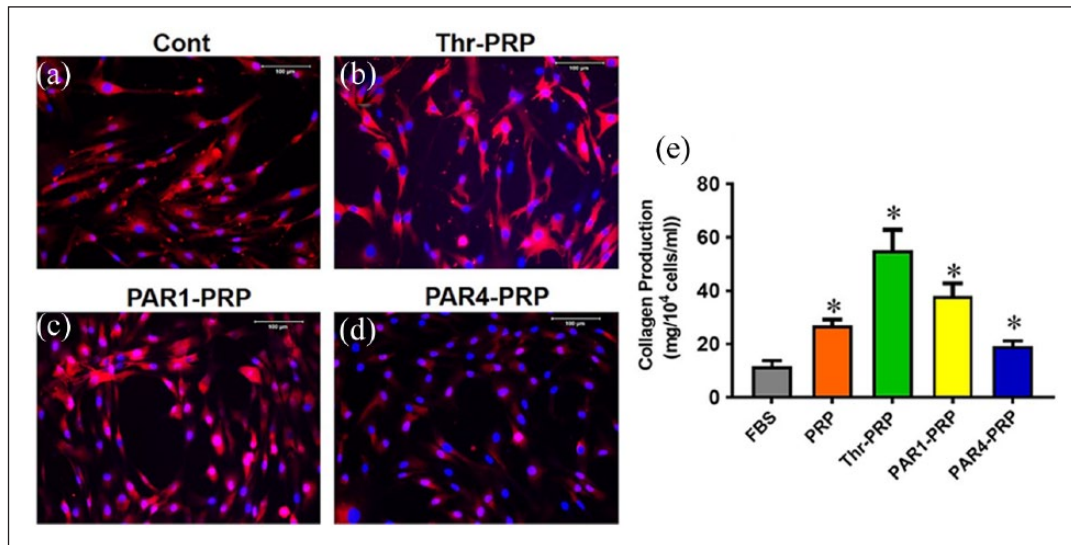


Figure 6. Differential effects of PAR1-PRP and PAR4-PRP on collagen type I. TSCs in all the three groups treated with 10% FBS (Cont), Thr-PRP, and PAR1-PRP are positively stained with collagen I (a, b, c); however, TSCs treated with PAR4-PRP express the smallest amount of collagen type I (d). Measurement of total collagen by Sircol assay shows that collagen production is about 2 times greater in PRP-, 5 times greater in thrombin-, 3 times in PAR1-, and only 1.6 times in PAR4-activated media. (e). * $p < 0.01$, with respect to control (FBS).

untreated control (red arrows, Figure 8(e) and (f)). The wound area treated with PAR4-PRP showed tendon-like tissues with well-organized collagen fibers and very few blood vessels (Figure 8(g) and (h)).

Safranin O and Fast Green staining further confirmed the above results. In the untreated control, a large unhealed wound area was clearly visible with no staining (Figure 9(a) and (b)). However, the healed tissue in the wound area treated with the thrombin-activated PRP was positively stained by Safranin O and Fast Green, indicating these scar tissues were cartilage-like tissues (red arrows, Figure 9(c) and (d)). Some vessel-like tissues were found in the wound area treated with PAR1-PRP, as well as some characteristic unhealed tissue as seen in the untreated control (Figure 9(e) and (f)). The wound area treated with PAR4-PRP showed tendon-like tissues with well-organized collagen fibers and very few blood vessels (Figure 9(g) and (h)).

Discussion

PLTs contain both pro- and anti-angiogenic regulatory proteins, meaning that they can stimulate or inhibit angiogenesis. The selective release of different factors is highly desirable for the proper healing of injured tissues, which could provide a more patient-specific treatment option in the case of PRP treatments. This study demonstrates that PAR1-PRP selectively released VEGF while PAR4-PRP released endostatin, which is consistent with the previous studies.^{11,12} Furthermore, we evaluated the differential effects of PAR1-PRP and PAR4-PRP on TSCs. Our data indicate that treatment of TSCs with both PAR1-PRP and

PAR4-PRP promoted their differentiation into tenocytes and enhanced cell proliferation. Interestingly, PAR1-PRP produced a “vessel-like” cellular pattern, whereas PAR4-PRP induced cellular organization in a parallel fashion. Moreover, PAR1-PRP produced more total collagen and enhanced collagen I gene expression in differentiated TSCs compared to PAR4-PRP. In addition, PAR1-PRP and PAR4-PRP differentially regulated MMP-1 and MMP-2 gene expression, further revealing that PAR1-PRP and PAR4-PRP exerts differential effects on TSCs. Finally, in our animal window defect model study, PAR1-PRP induced the formation of more blood vessels than PAR4-PRP, but the former produced disorganized scar tissues, whereas the latter resulted in more organized tissues. Taken together, these in vitro and in vivo findings show that PAR1-PRP and PAR4-PRP exert differential effects on TSCs and tendon healing.

One key aspect of tissue healing is angiogenesis, which is controlled by many stimulatory and inhibitory proteins including VEGF and endostatin. VEGF functions as an endothelial cell stimulator affecting angiogenesis that involves activation, migration, and proliferation of endothelial cells in pathological conditions,^{28–30} and is expressed during the proliferative and remodeling phases of tendon healing.^{31,32} Research into the role of VEGF in injury and wound healing has shown that the levels of VEGF expressed at the site of injury can have positive and negative effects. While increased VEGF promotes angiogenesis, the resulting increase in blood vessel formation also can result in scar formation in both fetal and adult tissues.³³ In addition, blocking VEGF by injection of anti-VEGF antibodies into scarred mice models neutralizes the effects of VEGF, resulting in

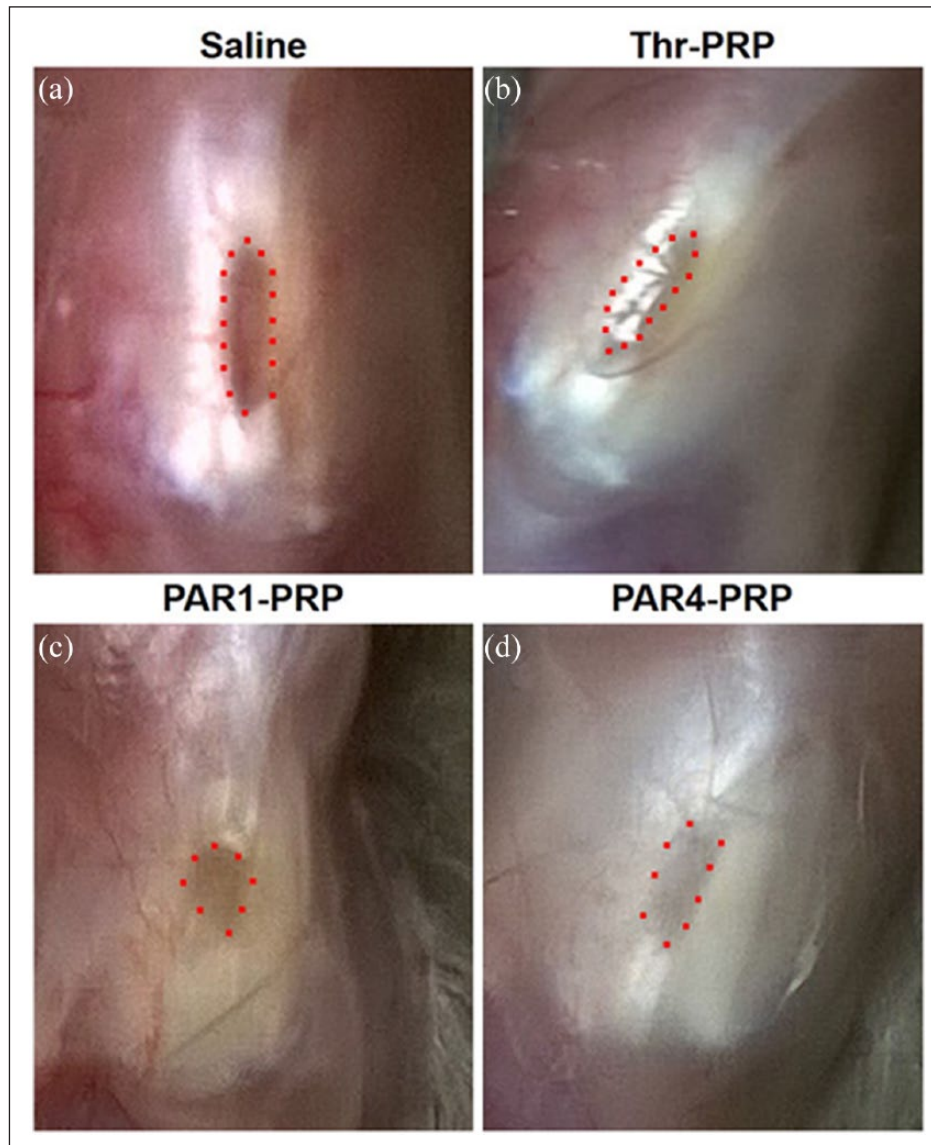


Figure 7. Differential wound healing effects of PAR1-PRP and PAR4-PRP in patellar tendon window defect model. (a) At 2 months post-injury, saline-treated control is still not healed, as evidenced by a large brownish healing tissue (red dots). (b) Thr-PRP-treated wound heals almost completely, with little brownish tissue. (c) Wounds treated with PAR1-PRP is not completely healed (dots indicate a small area of brown healing tissue) incomplete, with multiple blood vessel-like tissues. (d) PAR4-PRP-treated wound heals with much light brownish tissue, suggesting that the healed tissue is in a later stage. Moreover, fewer vessel-like tissues surround the wound area than those in the PAR1-PRP group.

decreased scarring and a more organized skin structure.³³ These previous findings complement our own. Since acute injuries are characterized by abundant levels of VEGF, treatment with PAR1-PRP could enhance the release of much higher levels of VEGF and thus could have deleterious effects such as increased scarring and poor healing. This suggests that PAR1-PRP is not appropriate for the treatment of acute tendon injury, which contains abundant VEGF already in wound site. PAR1-PRP, which enhances angiogenesis through the release of VEGF, might be better suited in a chronic tendon injury if healing is stalled due to the lack of sufficient formation of blood vessels.

On the other hand, treatment of acute injuries with PAR4-PRP would reduce the impact of excessive VEGF and hence angiogenesis, and consequently result in reduced scarring and formation of more organized tissues as seen in this study (Figures 8 and 9). Endostatin was discovered as a potent inhibitor of angiogenesis that specifically inhibits endothelial cell proliferation,³⁴ and is thought to be involved in the development and maintenance of an avascular zone in tendon.¹¹ Further research is certainly needed in this area.

As mentioned above, PAR1-PRP and PAR4-PRP also differ in their regulation of MMP-1 and MMP-2 gene expression. As remodelers of the extracellular matrix,

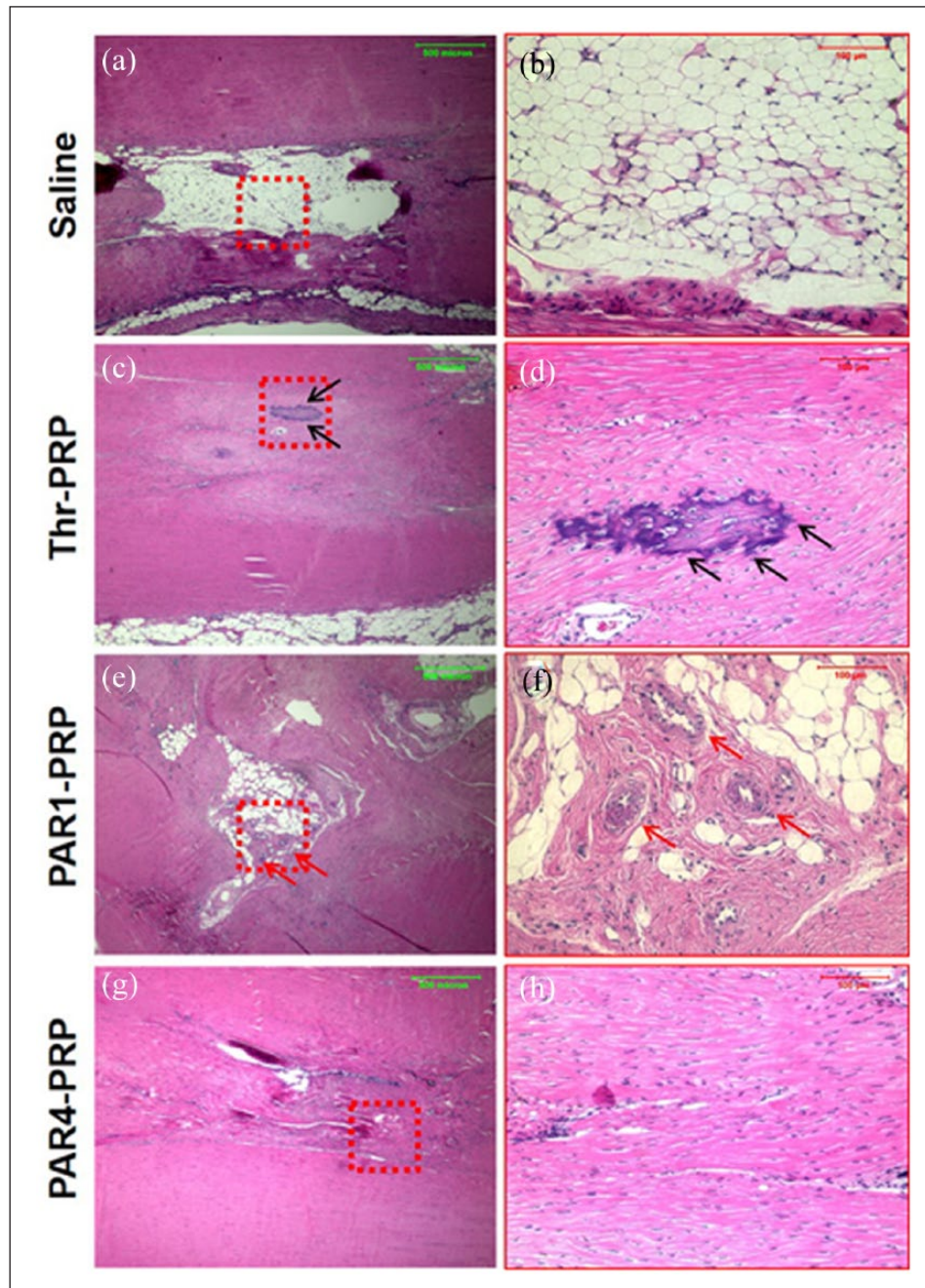


Figure 8. Differential wound healing effects of PAR1-PRP and PAR4-PRP assessed by H&E staining. (a) Wound without treatment (saline) shows large unhealed area 2 months' post-surgery (b) Enlarged red box in (a) clearly shows an unhealed wound. (c) Wound treated with thrombin-activated PRP shows healed wound with scar-like tissues (black arrows). (d) Enlarged red box in (c) showing healed wound with scar tissues with overgrowth (black arrows). (e) Wound treated with PAR1-activated PRP shows partially healed wound with blood vessel-like structures (red arrows). (f) Enlarged red box in (e) clearly shows vessel-like tissues (red arrows). (g) The wound area treated with PAR4-activated PRP shows tendon-like tissues with well-organized collagen fibers and very few blood vessels. (h) Enlarged red box in (g) clearly shows the wound area with well-organized collagen fibers and very few vessels compared with that treated with PAR1 (f). Green bars: 500 μm ; red bars: 100 μm .

MMP-1 and MMP-2 are both involved in the degradation of specific forms of collagen in wound healing and scarring, with expression of MMP-1 decreased and MMP-2 increased in excessively scarred tissues caused by excessive collagen deposition.⁹ Our data show that only PAR1-PRP resulted in

increased expression of MMP-1 as well as an increase in collagen I transcription levels and total collagen I protein production, while PAR4-PRP resulted in increased expression of MMP-2 with a lower increase in gene expression and total protein levels of collagen I. In short, in addition to

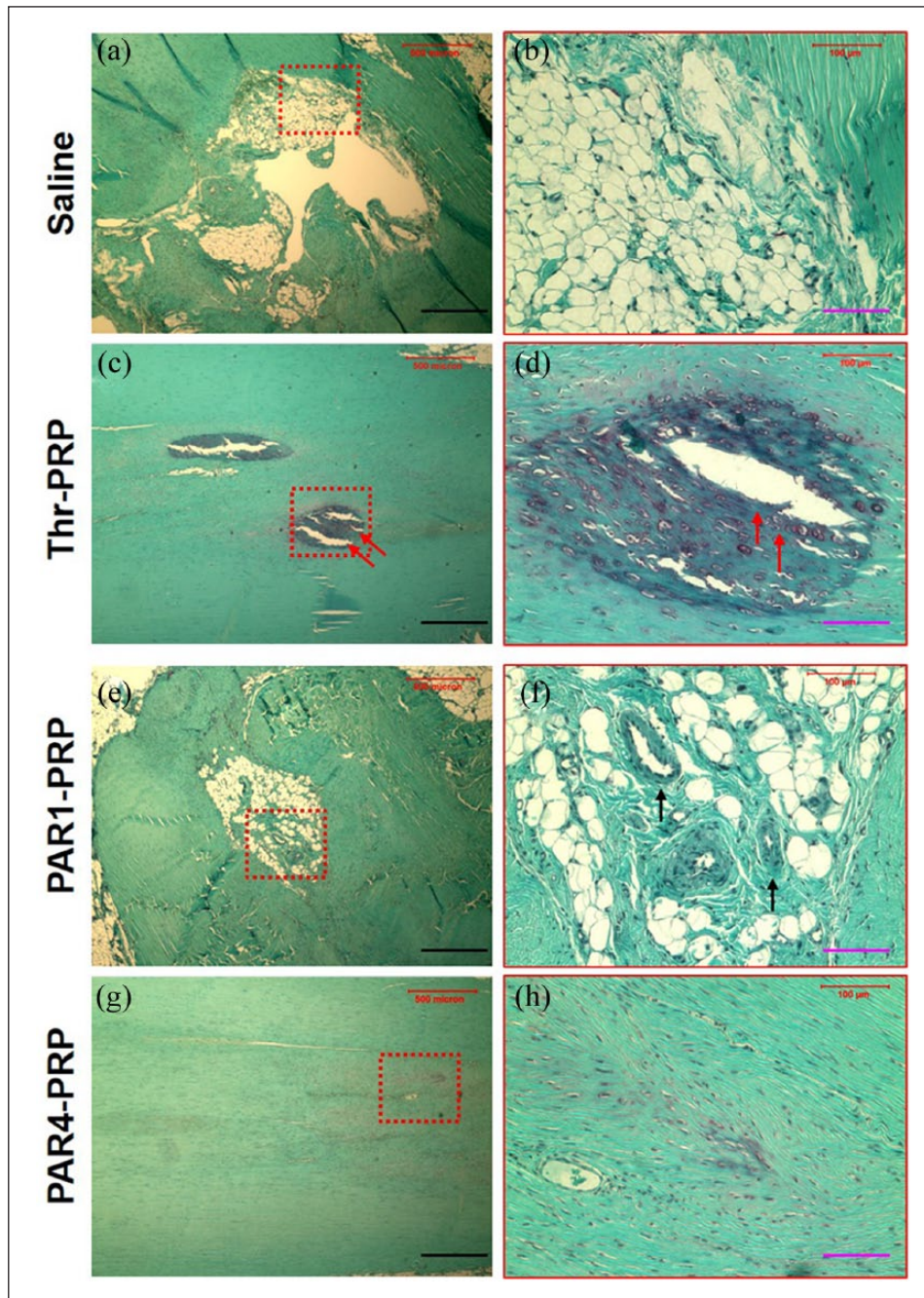


Figure 9. Differential wound healing effects of PAR1-PRP and PAR4-PRP assessed by Safranin O & Fast Green staining. (a) Wound without treatment (saline) shows a large unhealed area. (b) Enlarged red box in (a) showing a clear picture of unhealed area. (c) Wound treated with Thr-PRP shows a healed wound positively stained by Safranin O, indicating that they are cartilage-like tissues (red arrows). (d) Enlarged red box in (c) shows a clear picture of scar tissues (red arrows). (e) Wound treated with PAR1-PRP shows blood vessel-like tissues. (f) Enlarged red box in (e) showing vessel-like structures clearly (black arrows). (g) The wound area treated with PAR4-PRP shows tendon-like tissues with well-organized collagen fibers positively stained by Fast Green, and very few blood vessels. (h) Enlarged red box in (g) showing better organized collagen fibers compared with PAR1-PRP treatment. Black bars: 500 μm ; pink bars: 100 μm .

controlling angiogenesis with differential activation of PRP, there is also the possibility of modulating overall scar formation highlighting the potential risks and gains in using selectively activated PRP. Thus, these results further explain the better outcome of tendon healing (Figures 8 and 9) and support the use of PAR4-PRP to treat acute tendon injury.

The precise mechanisms by which PAR1-PRP and PAR4-PRP affect tendon wound healing are unknown, but they should be related to their effects on the TSC differentiation and resulting cell proliferation, which play an essential role in regeneration of injured tendons by proliferation and differentiation.^{16,35,36} Several studies

report improved healing in Achilles, patellar, and rotator cuff tendon injuries either by TSCs alone or in combination with PRP.^{17,20,21,37} Based on our in vitro results, we speculate that PAR1- and PAR4-PRP may regulate TSCs fate in vivo in a way that highly favors matrix synthesis augmented tendon healing and remodeling. Future studies should also address the application of TSCs stimulated with PAR1-PRP and PAR4-PRP in tendon injury models.

Conclusion

Selective activation of PRP using PAR1 and PAR4 has differential effects on differentiation, proliferation, and gene expression of TSCs as well as on wound healing of injured tendons, which is due to differential release of pro- and anti-angiogenic factors, VEGF and endostatin, respectively. The selective PRP activation may be applied in clinics based on acute or chronic injury to treat tendon injury successfully.

Acknowledgements

We thank Dr. Bhavani Thampatty for assistance in the preparation of this manuscript. J.Z. performed experiments, evaluated data, and drafted the manuscript. D.N. performed experiments, analyzed data, and drafted the manuscript. K.W. participated in the discussion and helped revise the manuscript. J.L.R. helped perform the experiments. M.V.H. participated in the discussion of this study and provided comments and suggestions on the experiments and formulation of the manuscript. J.H.W. conceived the study, provided feedback in the study design, experiments, and data analysis, and revised the manuscript.

Availability of data and materials

All the data can be obtained in this manuscript.

Declaration of conflicting interests

The author(s) declared no potential conflicts of interest with respect to the research, authorship, and/or publication of this article.

Funding


The author(s) disclosed receipt of the following financial support for the research, authorship, and/or publication of this article: This work was supported in part by NIH AR061395, AR065949, AR070340 (JHW), and Pittsburgh Pepper Center Pilot Study Funding P30AG024827.

Research ethics and patient consent

The protocol for obtaining blood samples was approved by the University of Pittsburgh Institutional Review Board (IRB#: PRO13090088). All patients gave written informed consent.

ORCID iDs

Daibang Nie  <https://orcid.org/0000-0003-3300-4537>

James H-C Wang  <https://orcid.org/0000-0001-7279-0679>

References

- Butler DL, Juncosa N and Dressler MR. Functional efficacy of tendon repair processes. *Annu Rev Biomed Eng* 2004; 6: 303–329.
- Proctor CS, Jackson DW and Simon TM. Characterization of the repair tissue after removal of the central one-third of the patellar ligament. An experimental study in a goat model. *J Bone Joint Surg Am* 1997; 79: 997–1006.
- Zhang J and Wang JH. The effects of mechanical loading on tendons—an in vivo and in vitro model study. *PLoS ONE* 2013; 8: e71740.
- Foster TE, Puskas BL, Mandelbaum BR, et al. Platelet-rich plasma: from basic science to clinical applications. *Am J Sports Med* 2009; 37: 2259–2272.
- Andia I, Sanchez M and Maffulli N. Tendon healing and platelet-rich plasma therapies. *Expert Opin Biol Ther* 2010; 10: 1415–1426.
- Boswell SG, Cole BJ, Sundman EA, et al. Platelet-rich plasma: a milieu of bioactive factors. *Arthroscopy* 2012; 28: 429–439.
- Zhou Y and Wang JH. PRP treatment efficacy for tendinopathy: a review of basic science studies. *Biomed Res Int* 2016; 2016: 9103792.
- Blair P and Flaumenhaft R. Platelet alpha-granules: basic biology and clinical correlates. *Blood Rev* 2009; 23: 177–189.
- Lee DE, Trowbridge RM, Ayoub NT, et al. High-mobility group box protein-1, matrix metalloproteinases, and vitamin D in keloids and hypertrophic scars. *Plast Reconstr Surg Glob Open* 2015; 3: e425.
- Pufe T, Petersen W, Tillmann B, et al. The angiogenic peptide vascular endothelial growth factor is expressed in foetal and ruptured tendons. *Virchows Arch* 2001; 439: 579–585.
- Pufe T, Petersen W, Kurz B, et al. Mechanical factors influence the expression of endostatin—an inhibitor of angiogenesis—in tendons. *J Orthop Res* 2003; 21: 610–616.
- Ma L, Perini R, McKnight W, et al. Proteinase-activated receptors 1 and 4 counter-regulate endostatin and VEGF release from human platelets. *Proc Natl Acad Sci U S A* 2005; 102: 216–220.
- Chatterjee M, Huang Z, Zhang W, et al. Distinct platelet packaging, release, and surface expression of proangiogenic and antiangiogenic factors on different platelet stimuli. *Blood* 2011; 117: 3907–3911.
- Italiano JE Jr, Richardson JL, Patel-Hett S, et al. Angiogenesis is regulated by a novel mechanism: pro- and antiangiogenic proteins are organized into separate platelet alpha granules and differentially released. *Blood* 2008; 111: 1227–1233.
- De Candia E. Mechanisms of platelet activation by thrombin: a short history. *Thromb Res* 2012; 129: 250–256.
- Zhang J and Wang JH. Platelet-rich plasma releasate promotes differentiation of tendon stem cells into active tenocytes. *Am J Sports Med* 2010; 38: 2477–2486.
- Ni M, Lui PP, Rui YF, et al. Tendon-derived stem cells (TDSCs) promote tendon repair in a rat patellar tendon window defect model. *J Orthop Res* 2012; 30: 613–619.
- Lui PP and Chan KM. Tendon-derived stem cells (TDSCs): from basic science to potential roles in tendon pathology and tissue engineering applications. *Stem Cell Rev* 2011; 7: 883–897.

19. Komatsu I, Wang JH, Iwasaki K, et al. The effect of tendon stem/progenitor cell (TSC) sheet on the early tendon healing in a rat Achilles tendon injury model. *Acta Biomater* 2016; 42: 136–146.
20. Chen L, Liu JP, Tang KL, et al. Tendon derived stem cells promote platelet-rich plasma healing in collagenase-induced rat achilles tendinopathy. *Cell Physiol Biochem* 2014; 34: 2153–2168.
21. Chen L, Dong SW, Liu JP, et al. Synergy of tendon stem cells and platelet-rich plasma in tendon healing. *J Orthop Res* 2012; 30: 991–997.
22. Zhang J, Keenan C and Wang JH. The effects of dexamethasone on human patellar tendon stem cells: implications for dexamethasone treatment of tendon injury. *J Orthop Res* 2013; 31: 105–110.
23. Zhang JY and Wang JHC. Characterization of differential properties of rabbit tendon stem cells and tenocytes. *BMC Musculoskeletal Disord* 2010; 11: 10.
24. Theret N, Lehti K, Musso O, et al. MMP2 activation by collagen I and concanavalin A in cultured human hepatic stellate cells. *Hepatology* 1999; 30: 462–468.
25. Konttinen YT, Ainola M, Valleala H, et al. Analysis of 16 different matrix metalloproteinases (MMP-1 to MMP-20) in the synovial membrane: different profiles in trauma and rheumatoid arthritis. *Ann Rheum Dis* 1999; 58: 691–697.
26. Zhang J, Pan T, Im HJ, et al. Differential properties of human ACL and MCL stem cells may be responsible for their differential healing capacity. *BMC Med* 2011; 9: 68.
27. Zhang J, Yuan T and Wang JH. Moderate treadmill running exercise prior to tendon injury enhances wound healing in aging rats. *Oncotarget* 2016; 7: 8498–8512.
28. Ferrara N and Davis-Smyth T. The biology of vascular endothelial growth factor. *Endocr Rev* 1997; 18: 4–25.
29. Ferrara N and Keyt B. Vascular endothelial growth factor: basic biology and clinical implications. *EXS* 1997; 79: 209–232.
30. Zachary I. Vascular endothelial growth factor. *Int J Biochem Cell Biol* 1998; 30: 1169–1174.
31. Gelberman RH, Khabie V and Cahill CJ. The revascularization of healing flexor tendons in the digital sheath. A vascular injection study in dogs. *J Bone Joint Surg Am* 1991; 73: 868–881.
32. Boyer MI, Watson JT, Lou J, et al. Quantitative variation in vascular endothelial growth factor mRNA expression during early flexor tendon healing: an investigation in a canine model. *J Orthop Res* 2001; 19: 869–872.
33. Wilgus TA, Ferreira AM, Oberyzyzn TM, et al. Regulation of scar formation by vascular endothelial growth factor. *Lab Invest* 2008; 88: 579–590.
34. O'Reilly MS, Boehm T, Shing Y, et al. Endostatin: an endogenous inhibitor of angiogenesis and tumor growth. *Cell* 1997; 88: 277–285.
35. Zhang J and Wang JH. Mechanobiological response of tendon stem cells: implications of tendon homeostasis and pathogenesis of tendinopathy. *J Orthop Res* 2010; 28: 639–643.
36. Zhang J, Pan T, Liu Y, et al. Mouse treadmill running enhances tendons by expanding the pool of tendon stem cells (TSCs) and TSC-related cellular production of collagen. *J Orthop Res* 2010; 28: 1178–1183.
37. Chen JM, Willers C, Xu J, et al. Autologous tenocyte therapy using porcine-derived bioscaffolds for massive rotator cuff defect in rabbits. *Tissue Eng* 2007; 13: 1479–1491.